Terahertz Time-Domain Observation of Spin Reorientation in Orthoferrite $ErFeO_3$ through Magnetic Free Induction Decay

Keita Yamaguchi, Takayuki Kurihara, Yasuo Minami,* Makoto Nakajima,† and Tohru Suemoto
Institute for Solid State Physics, The University of Tokyo, Kashiwa, Chiba 277-8581, Japan
(Received 23 November 2012; published 26 March 2013)

Terahertz time domain spectroscopy was performed on orthoferrite $ErFeO_3$. Through the emission from the two magnetic resonance modes, we succeeded in observing the spin reorientation transition. Depending on the orientation of the single crystal, the reorientation can be detected as either mode switching between the two modes or polarization change of the emission. This method enables picosecond resolved observation of the reorientation without disturbances such as electronic excitation and heating, and it is expected to open the doorway to observe ultrafast reorientation with the terahertz pulse.

DOI: 10.1103/PhysRevLett.110.137204 PACS numbers: 75.78.Jp, 75.30.Kz, 76.50.+g, 78.20.Ls

Ultrafast optical control of spins is one of the promising methods for development in spintronics and information processing technologies. For this reason, a number of studies on such control with a high intensity femtosecond visible laser has been reported [1–11]. Although these experiments revealed interesting magnetic phenomena such as an ultrafast manipulation of spins through thermally induced spin reorientation transition [1–3], ultrafast demagnetization in colossal magnetoresistance manganites [4], the inverse Faraday effect [2,3,5–9], the inverse Cotton-Mouton effect [5,6], and the magnetic difference frequency generation [10,11], in an applicative point of view, the generation of excess heat and unwanted electronic excitation may be a hindrance. On the other hand, direct impulsive excitation of spin precession motion by means of a magnetic field component of the terahertz (THz) pulse [12–14] is free from electronic excitations because of small photon energy in this spectral region. In addition, since the pulse energy of the THz pulse emitted from photoconductive antennas excited with a femtosecond oscillator is typically on the order of femtojoule, thermal effect is also negligible. The excitation of precession by the THz magnetic field is described by the Bloch equation

$$\frac{d\boldsymbol{M}}{dt} = \gamma \boldsymbol{M} \times (\boldsymbol{H}_{\mathrm{THz}} + \boldsymbol{H}_{\mathrm{eff}}),$$

where $\boldsymbol{M}$, $\boldsymbol{H}_{\mathrm{THz}}$, $\boldsymbol{H}_{\mathrm{eff}}$, and γ are the magnetic moment, THz magnetic field component, effective magnetic field, and gyromagnetic ratio, respectively. As a THz magnetic pulse enters, spins are tilted because of the torque applied by the magnetic pulse. Tilted from their equilibrium orientation, spins start to coherently precess in the effective magnetic field. Because of this motion of spins, magnetic dipole radiation is induced and can be detected as free induction decay signals. Thus, by performing a THz time domain spectroscopy (TDS), both excitation and sub-picosecond resolution real time observation of spin precession can be done simultaneously.

Some orthoferrites, $ErFeO_3$ for example, are known to show temperature-induced phase transition called spin reorientation transition, where spins rotate 90 degrees from one direction to another [15–18]. To the best of our knowledge, an observation of the spin reorientation transition with the THz TDS method has not been reported in the past. Here, we propose the observation method of spin reorientation with the THz TDS method, and we demonstrated this with $ErFeO_3$. The method used in this study is expected to enable detection of spin reorientation with picosecond time resolution and may be applied for studying the underlying mechanism of ultrafast spin reorientation owing to inertia driven spin switching [9] and ultrafast heating [1–3], which are a part of the intriguing phenomena found by the spin manipulation with the femtosecond laser.

Orthoferrite $RFeO_3$ (R denotes Y and rare-earth-metal elements) is classified as a weak ferromagnet where antiferromagnetically ordered spins cant toward one direction and have a macroscopic magnetization. $ErFeO_3$ shows weak ferromagnetism below Néel temperature $T_N = 643$ K [16]. In this weak ferromagnetic phase, orthoferrites have two optically active magnetic resonance modes in the sub-THz region, namely quasiferromagnetic mode (F mode) and quasiantiferromagnetic mode (AF mode). F mode resonance can be interpreted as a precession of the macroscopic magnetization. AF mode, on the other hand, can be seen as a fluctuation in magnitude of the magnetization. These two magnetic resonances are known to be excited only by a magnetic field pulse with a specific polarization: magnetic field perpendicular to the magnetization for exciting the F mode, and magnetic field parallel to the magnetization for the AF mode [19,20]. In the case of $ErFeO_3$, the resonant frequency for F and AF modes at room temperature are 0.377 THz and 0.673 THz, respectively [18]. The spin reorientation transition in $ErFeO_3$ is described in Fig. 1. In the temperature range higher than 96 K (high temperature phase), the easy axis of Fe^{3+} spins is in the a axis and the macroscopic

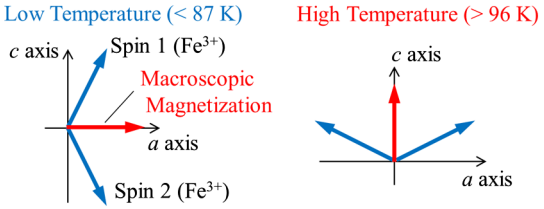

FIG. 1 (color online). Schematic of spin configurations in $ErFeO_3$ for high-temperature and low-temperature phases. The blue arrows indicate Fe^{3+} spins, and the red arrows indicate macroscopic magnetization, which results from canting of the Fe^{3+} spins.

magnetization is parallel to the c axis. At 87 K or lower (low temperature phase), the c axis becomes the easy axis with macroscopic magnetization in the a axis direction. Between 87 and 96 K, the easy axis continuously rotates between the a axis and the c axis [15–18].

Transmission-type THz TDS measurements were conducted at various temperatures. For generation and detection of the THz pulse, low temperature grown GaAs photoconductive antennas that emit and detect THz waves with a horizontally polarized electric field component were used. The antennas were excited using mode-locked Ti: sapphire femtosecond laser pulses (12 fs, center wavelength at 800 nm, and repetition rate of 75 MHz). THz signals in the polarizations perpendicular to the antenna were obtained from the difference of the signals in $\pm 45°$ polarization angles [12,13]. Two kinds of samples were used in this study. One is a c-cut plane parallel plate of single crystal $ErFeO_3$ grown by the floating zone method, hereafter referred to as the c-plane sample. The directions of the crystal axes were determined by x-ray Laue analysis. The thickness was approximately 1.3 mm. The other sample is a 1.6 mm thick sintered pellet of $ErFeO_3$ powder. The average diameter of grains in the pellet was about 8 μm. Both samples were fixed onto a 4 mm diameter metal aperture during the measurements. The samples were magnetized before each measurement and have residual magnetization. No static magnetic field was applied to the samples during the measurements. In the measurements conducted below room temperature, a cold finger cryostat (Oxford Instruments) was used.

Figure 2(a) shows the transmitted temporal waveforms of the THz pulse obtained with the c-plane single crystal sample magnetized along the c axis. The measurement was performed at room temperature. In the polarization parallel to the incident THz pulse, the main pulse of the THz pulse is followed by an oscillating component that corresponds to magnetic dipole emission because of magnetic resonance. In the perpendicular polarization, only the oscillating component owing to the resonance can be observed without overlapping of the THz main pulse. By inverting the direction of the magnetic pole, the phase of the oscillation in perpendicular polarization is shifted by π,

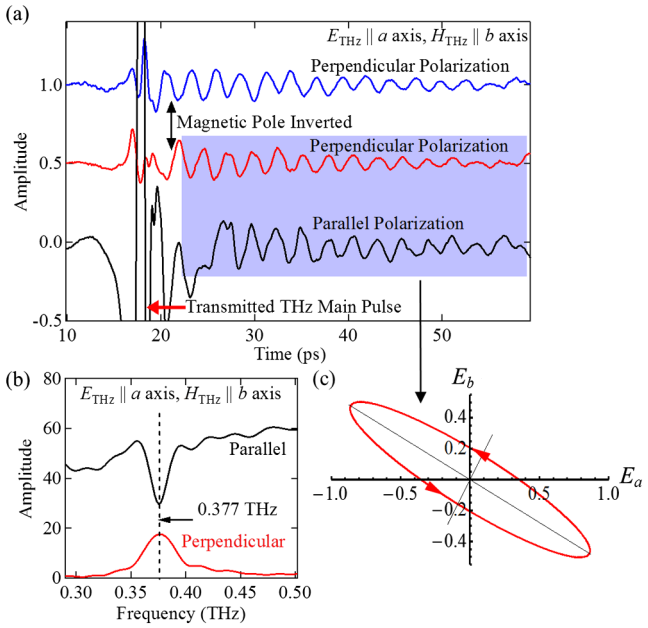

FIG. 2 (color online). (a) Temporal waveforms of transmitted THz wave through c plane $ErFeO_3$ single crystal. (b) Spectra obtained by Fourier transformation of temporal waveforms in (a). (c) Electric field component trajectory of emission at 0.377 THz calculated from (a).

meaning that the helicity change between the left hand circular emission and the right hand circular emission occurred. This explains that these oscillations are free induction decay signals emitted from the precession of macroscopic magnetization. Because the emissions in perpendicular polarization from antiparallel magnetic domains cancel one another, the perpendicular component can be detected only when the sample is magnetized. Spectra obtained from Fourier transformation of the temporal waveforms with a time window from 0 ps to 60 ps in Fig. 2(a) are shown in Fig. 2(b). Reflecting the oscillations in temporal waveforms, a dip and a peak appear in the parallel component and the perpendicular component, respectively. Both structures appear at around 0.377 THz, which coincides with the F mode resonance at room temperature, indicating that the F mode resonance is impulsively excited by the THz pulse. Note that since single crystal $ErFeO_3$ is a birefringent medium (in the THz region), the optical path length in the a axis and the b axis are different. In our measurement, the refractive indices in the THz region were $n_a = 5.1$ and $n_b = 4.9$. For this reason, the phase difference between parallel and perpendicular polarization is not $\pi/2$. Figure 2(c) shows the radiation trajectory of emission at 0.377 THz obtained from the ellipticity and rotation angle computed with the well-known formulas [21]. The principal axes of elliptic radiation are not parallel to the a axis and the b axis because of the birefringence. The reason that the radiation is elliptic is threefold. First of all, the F mode precession

itself is elliptic [19]. Second, phase mismatch because of the birefringent effect between the incident THz pulse and the emission in perpendicular polarization also degrades the emission in perpendicular polarization. Finally, while the emissions from antiparallel domains add up in parallel polarization, they cancel out in perpendicular polarization. Therefore, the amplitude of the emission in parallel polarization is proportional to the saturation magnetization I_s, whereas in perpendicular polarization, it is proportional to the residual magnetization I_r.

Next, temperature dependence of resonant frequencies for F and AF modes were obtained (Fig. 3). While the AF mode frequency changes gradually, the F mode frequency changes significantly near the reorientation temperature. These behaviors of the frequencies are described by

$$(\hbar\omega_{\mathrm{FM}})^2 = [4E/(2S)^2][(A_{xx} - A_{zz})\cos 2\theta - 4K_4 \cos 4\theta],$$

$$(\hbar\omega_{\mathrm{AFM}})^2 = [4E/(2S)^2]\left[\frac{1}{2}(A_{xx} + A_{zz}) + \frac{1}{2}(A_{xx} - A_{zz})\cos 2\theta - K_4 \cos 4\theta\right],$$

where A_{xx} and A_{zz} are the second order anisotropy energy, K_4 is the fourth order anisotropy energy, θ is the angle between the c axis and the weak ferromagnetic moment, E is the exchange constant, and S is the sublattice magnetization magnitude [17]. Near the spin reorientation temperature region, the term $(A_{xx} - A_{zz})$ approaches zero and the F mode frequency softens. In the AF mode frequency, the term $(A_{xx} + A_{zz})$, which is 2 orders of magnitude larger than the fourth order anisotropy, is dominant and suppresses the softening of the AF mode frequency, resulting in the gradual change observed in the measurement. The temperature dependence shown here also agrees with the resonant frequency obtained with the backward wave oscillator [18]. No notable difference between frequencies in the sintered pellet and the single crystal sample was present.

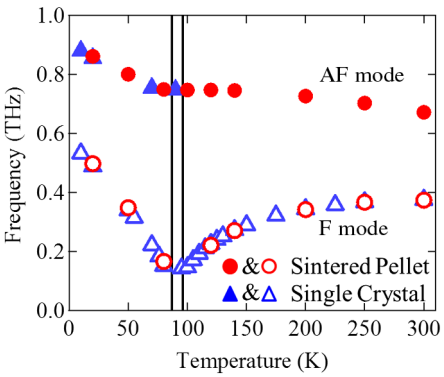

FIG. 3 (color online). Temperature dependence of F and AF mode resonant frequencies in $ErFeO_3$. Circle markers show frequencies obtained with the sintered pellet, and triangle markers show frequencies in a single crystal sample with (001) surface. Two vertical lines indicate higher and lower transition temperatures at 96 K and 87 K.

Spectra in Fig. 4(a) show peaks that correspond to radiation owing to magnetic resonance excited with the THz magnetic field parallel to the a axis in the c-plane single crystal. As described in Fig. 4(b), in the high temperature phase (250 K), the magnetic field component of the THz pulse is perpendicular to the macroscopic magnetization, resulting in excitation of the F mode. As the sample goes through the reorientation transition into the low temperature phase, H_{THz} polarized in the a-axis direction becomes parallel to the magnetization, resulting in excitation of the AF mode resonance. The spectra in Fig. 4(a) clearly reflect this behavior, which verifies that the reorientation phase transition can be detected through magnetic resonance mode switching. In addition, returning the temperature to 250 K simply caused the radiation mode to switch back to the F mode, which shows that this switching is a reversible phenomenon. Because this change occurs in parallel polarization, this behavior can also be observed in the absence of the residual magnetization. In the temporal waveforms, observation of the half-cycle of the oscillation is sufficient for distinguishing the F mode and AF mode resonance. Therefore, by focusing on the existence of the AF mode (oscillation period $T_{AF} =$ 1.33 ps), the phase of the spins can be determined with 0.67 ps resolution.

Next, the magnetized c-plane sample was excited with the $H_{\mathrm{THz}}||b$ incident THz pulse. Figure 5(a) shows intensity spectra of oscillating components obtained in this configuration. At the high temperature phase, Fig. 5(a) shows that the F mode radiation exists in both parallel and perpendicular polarization. As depicted in Fig. 5(b), this is because the F mode precession in the high temperature phase takes place inside the a-b plane. Magnetic

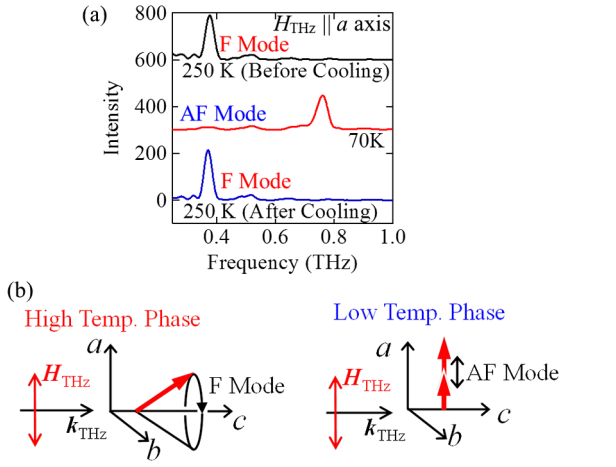

FIG. 4 (color online). (a) Intensity spectra of oscillatory components obtained with $H_{\mathrm{THz}}||a$-axis THz pulse excitation. (b) The relation of the incident THz polarization with excited resonance modes in each phase.

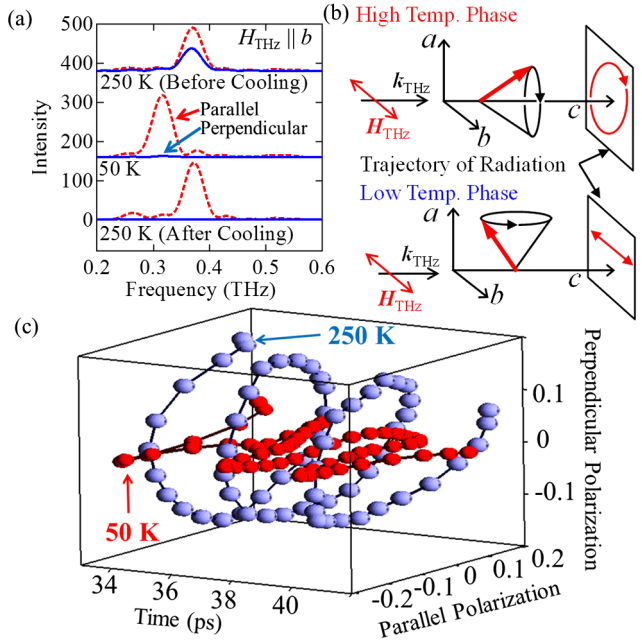

FIG. 5 (color online). (a) Fourier spectra of oscillatory components in waveforms obtained from $H_{THz} \| b$-axis excitation. The red dashed line and the blue line show the oscillation in the polarization parallel and perpendicular to the incident THz pulse, respectively. (b) Schematic of spin precession motion and magnetic field component trajectory of radiation emitted from the precession in high temperature and low temperature phases. (c) Three-dimensional trajectory plot of temporal waveforms at 250 K and 50 K.

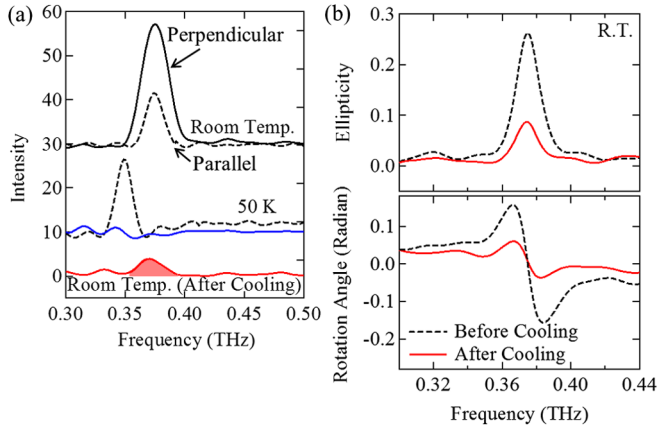

FIG. 6 (color online). (a) Spectra obtained from Fourier transformation of waveforms in perpendicular polarization with a magnetized sintered pellet. The dashed spectra show the oscillatory component in the parallel polarization (arbitrary unit) for each temperature. (b) Magneto-optical spectra of the pellet sample at room temperature before and after cooling.

dipole radiation with the wave vector in the c-axis direction, which is obtained in this experimental setup, reflects the motion of magnetic dipole in the a-b plane, leading to observation of elliptically polarized emission in the high temperature phase. At 50 K, although the spectrum in parallel polarization clearly shows the F mode peak, Fig. 5(a) shows that no peak is present in perpendicular polarization. This is because the precession occurs in the b-c plane at the low temperature phase and the observed emission with a wave vector in the c axis becomes linearly polarized, as illustrated in Fig. 5(b). The three-dimensional trajectory plot of temporal waveforms also clearly show that emission in 250 K is elliptic while the emission in 50 K is linearly polarized [Fig. 5(c)]. For the ease to see, the phase shift owing to the birefringence was compensated with an offset of 0.3π in perpendicular polarization, which is expected from an estimation also used in Ref. [13]. With no static magnetic field along the c axis present, when the sample's phase is returned to the high temperature phase again, the oscillation in perpendicular polarization does not reappear [Fig. 5(a)], meaning that the residual magnetization is lost during the reorientation. Thus, it should be noted that in the low temperature phase, beside the magnetic domain with macroscopic magnetization in the $+a$ direction, which is illustrated in Fig. 5(b), an equivalent number of domains with macroscopic magnetization in the $-a$ direction also exists.

Observation of radiation in perpendicular polarization was also done with the magnetized sintered pellet sample. As Fig. 6(a) shows, phase transition into the low temperature phase results in the disappearance of the radiation, which is consistent with the result in the single crystal sample. However, returning the sample's phase into the high temperature phase revealed that a small portion of the F mode emission remains. This shows that the residual magnetization in the sintered pellet is not completely lost even after the spin reorientation transition. In Fig. 6(b), the ellipticity and rotation angle spectra at 250 K before and after cooling clearly show that the elliptic emission observed before cooling is partially recovered after cooling. As the sign of the ellipticity indicates, the helicity of emission in room temperature does not change even after cooling. Therefore, a memory effect that records the direction of some portion of the magnetic domains seems to exist. From the magnetic field strength required to magnetize the samples, the coercive field of the pellet sample is estimated to be over 500 kA/m, whereas in the single crystal, it is below 10 kA/m. Considering the large difference in the coercive field, this memory effect may be ascribed to various reasons such as pinning of magnetic domain walls owing to defects in the microcrystal and stress induced from lattice defects and grain boundaries, and thus, further investigations on the origin of the effect are required.

To summarize, THz TDS measurement was performed on orthoferrite $ErFeO_3$. The magnetic field component of the THz pulse acted as a half-cycle magnetic pulse and impulsively excited coherent precession motion of spins. We have successfully observed the spin reorientation transition in $ErFeO_3$ through changes in precession frequency and changes in polarization of radiation from the spins.

Since these methods offer the ability for resolving the phase transition within a picosecond without induction of unnecessary disturbances such as electronic excitation and heating, the results introduced here open a way to observe ultrafast reorientation dynamics with THz TDS measurement.

This work has been supported by JSPS Grant-in-Aid (Grants No. 23244063, No. 23686012, No. 23760045, and No. 11J02179) and from The Murata Science Foundation. K. Y. is grateful for the support from the JSPS Research Fellowship.

*Present address: Department of Physics, Faculty of Engineering, Yokohama National University, Yokohama 240-8501, Japan.

†Present address: Graduate School of Science, Chiba University, Chiba 263-8522, Japan.

[1] A. V. Kimel, A. Kirilyuk, A. Tsvetkov, R. V. Pisarev, and Th. Rasing, Nature (London) **429**, 850 (2004).

[2] J. A. de Jong, A. V. Kimel, R. V. Pisarev, A. Kirilyuk, and Th. Rasing, Phys. Rev. B **84**, 104421 (2011).

[3] J. A. de Jong, I. Razdolski, A. M. Kalashnikova, R. V. Pisarev, A. M. Balbashov, A. Kirilyuk, Th. Rasing, and A. V. Kimel, Phys. Rev. Lett. **108**, 157601 (2012).

[4] R. D. Averitt, A. I. Lobad, C. Kwon, S. A. Trugman, V. K. Thorsmølle, and A. J. Taylor, Phys. Rev. Lett. **87**, 017401 (2001).

[5] J. Nishitani, K. Kozuki, T. Nagashima, and M. Hangyo, Appl. Phys. Lett. **96**, 221906 (2010).

[6] R. Iida, T. Satoh, T. Shimura, K. Kuroda, B. A. Ivanov, Y. Tokunaga, and Y. Tokura, Phys. Rev. B **84**, 064402 (2011).

[7] J. Nishitani, T. Nagashima, and M. Hangyo, Phys. Rev. B **85**, 174439 (2012).

[8] A. V. Kimel, A. Kirilyuk, P. A. Usachev, R. V. Pisarev, A. M. Balbashov, and Th. Rasing, Nature (London) **435**, 655 (2005).

[9] A. V. Kimel, B. A. Ivanov, R. V. Pisarev, P. A. Usachev, A. Kirilyuk, and Th. Rasing, Nat. Phys. **5**, 727 (2009).

[10] T. Higuchi, N. Kanda, H. Tamaru, and M. Kuwata-Gonokami, Phys. Rev. Lett. **106**, 047401 (2011).

[11] N. Kanda, T. Higuchi, H. Shimizu, K. Konishi, K. Yoshioka, and M. Kuwata-Gonokami, Nat. Commun. **2**, 362 (2011).

[12] M. Nakajima, A. Namai, S. Ohkoshi, and T. Suemoto, Opt. Express **18**, 18 260 (2010).

[13] K. Yamaguchi, M. Nakajima, and T. Suemoto, Phys. Rev. Lett. **105**, 237201 (2010).

[14] T. Kampfrath, A. Sell, G. Klatt, A. Pashkin, S. Mährlein, T. Dekorsy, M. Wolf, M. Fiebig, A. Leitenstorfer, and R. Huber, Nat. Photonics **5**, 31 (2011).

[15] R. L. White, J. Appl. Phys. **40**, 1061 (1969).

[16] H. P. J. Wijn, in *5.5.8.11 ErFeO{3} Compounds In 5.5.8 RFeO{3} Compounds* (Springer-Verlag, Berlin, 1994), pp. 138–142.

[17] S. M. Shapiro, J. D. Axe, and J. P. Remeika, Phys. Rev. B **10**, 2014 (1974).

[18] G. V. Kozlov, S. P. Lebedev, A. A. Mukhin, A. S. Prokhorov, I. V. Fedorov, A. M. Balbashov, and I. Y. Parsegov, IEEE Trans. Magn. **29**, 3443 (1993).

[19] G. F. Herrmann, J. Phys. Chem. Solids **24**, 597 (1963).

[20] A. A. Mukhin, M. Biberacher, A. Pimenov, and A. Loidl, J. Magn. Reson. **170**, 8 (2004).

[21] M. Born and E. Wolf, *The Principle of Optics* (Cambridge University Press, London, 1999).